Differential Evolution-based Optimization of Corn Stalks Black Liquor Decolorization with Active Carbon Adsorption and TiO2 Promoted Photochemical Degradation

Nechita Teodor
Gheorghe Asachi Technical University of Iași
Suditu Dan
Gheorghe Asachi Technical University of Iași
Puițel Cătălin
Gheorghe Asachi Technical University of Iași
Elena Niculina Dragoi (elenan.dragoi@gmail.com)
Gheorghe Asachi Technical University of Iași

Research Article

Keywords: black liquor, decolorization, modeling, optimization

Posted Date: July 6th, 2021

DOI: https://doi.org/10.21203/rs.3.rs-658361/v1

Abstract

In this work, the active carbon adsorption and TiO_2 promoted photochemical degradation of black liquor decolorization were studied through experimental analysis (planned using Design of Experiments), modelling and optimization (with Response Surface Method and Differential Evolution). The aim is to highlight the importance of optimization methods for increasing process efficiency. For active carbon adsorption the considered process parameters were: quantity of active carbon, dilution, and contact time; for TiO_2 promoted photochemical degradation the process parameters were: TiO_2 concentration, UV path length and irradiation time. The determined models had an R squared of 93.82% for active carbon adsorption and of 92.82% for TiO2 based degradation. In the optimization phase, for active carbon, an improvement from 81.27–100% and for TiO2-based degradation from 36.63–46.83% was obtained. These results show that the experiments and the subsequent standard RSM optimization data can be further improved, leading to better performance.

1. Introduction

Black liquor (BL) is definitely one the most known byproduct of the pulp and paper industry, highly appreciated for its caloric value as industrial fuel and correspondingly unattractive from the environmental point of view (Zaied and Bellakhal 2009). Both the chemical content and the color of the black liquor containing effluents are of major concern regarding environmental protection. Therefore, numerous physicochemical treatments and decolorization methods have been proposed over the years. Examples include: coagulation and precipitation (Ganjidoust et al. 1997; Garg et al. 2010), electrocoagulation (Shankar et al. 2014; Azadi Aghdam et al. 2016), adsorption (Mohan and Karthikeyan 1997), wet oxidation (Garg et al. 2007), ozonation (Kreetachat et al. 2007; De Los Santos Ramos et al. 2009), photochemical degradation (Kansal et al. 2008), biodegradation and other advanced oxidation processes (Baycan Parilti and Akten 2011; Merayo et al. 2013), each having its own advantages and drawbacks. In the context of technical progress of pulp and paper industry and with the continuous tightening of the environmental standards and regulations, these methods must continually prove their economical and practical viability. Thus, great efforts are made to enhance and to optimize the existing treatment methods, to find the optimal operational parameters in order to increase efficiency and reduce costs (Darvishmotevalli et al. 2019; Zhang et al. 2019; Ghasemi et al. 2020; Kloch and Toczyłowska-Mamińska 2020; Panepinto et al. 2020; Shomar et al. 2020; Wang et al. 2020; Zhou et al. 2020).

One of the classical optimization approaches used for studies regarding the degradation and decolorization of pulp and paper effluents (Baycan Parilti and Akten 2011; Torrades et al. 2011; Kim 2016; Subramonian et al. 2017) is Response Surface Method (RSM) based on central composite design (CCD), proposed in the 60’s by Box and Hunter (Box and Hunter 1957). Currently, the outstanding progress of computational science and engineering allows the application of a variety of algorithms for optimizing real-world problems. The main two groups these algorithms can be classified into are: deterministic and stochastic (Mirjalili et al. 2017). The difference between the two consists in the characteristics of the solutions obtained. If starting from the same point, the deterministic approaches will always provide the

same solution, while the stochastic ones will generate different solutions (that can be distributed in the search space or tightly packed together). Due to their effectiveness and general applicability, the stochastic approaches are often used as alternatives to the classical optimization variants. Therefore, in this work, along RSM, a stochastic approach represented by a bio-inspired metaheuristic - Differential Evolution (DE) (Storn and Price 1995)- is used as an alternative to the RSM optimization.

The goal of the present work is to twofold: i) study and identify, using both classical and alternative optimization techniques, the optimal reaction condition for decolorization of a black liquor obtained in laboratory from corn stalks; and ii) demonstrate that the classical approaches, through a careful process analysis and using state of the art computational approaches can be improved to keep with the novel decolorization processes. To this means, a three-step procedure is used:

i) experimental (where an experimental plan is set-up and followed). Two extensively studied decolorization procedures (Zhang and Chuang 2001; Ksibi et al. 2003; Chang et al. 2004; Ugurlu et al. 2005; Kansal et al. 2008) were selected and used in lab-scale experiments: active carbon decolorization (ACD) and TiO_2 promoted photochemical decolorization (PCD). The role of specific key parameters and their interactions were evaluated for each procedure;

ii) modelling (where data gathered from the previous step is statistically modeled in order to determine a set of mathematical relations that can describe the processes). The method used to perform this step is represented by RSM;

iii) optimization (where the previously determined model in combination with an optimizer is used to identify the optimal process parameters). The algorithm used to perform the optimization is represented by DE.

The chosen decolorization methods (ACD and PCD) were selected based on their simplicity, reduced cost and ease of implementation. The aim is not to prove which of the two processes is better but to demonstrate that novel computational techniques can provide additional strategies to improve their efficiency beyond the standard performance levels reported so far. To the author’s knowledge combination of ACD and PCD with the modelling/optimization techniques (RSM and DE) have never been studied in such manner before.

2. Materials And Methods

2.1 Materials

The black liquor used in the study was obtained from a laboratory scale system for cellulose production and it was based on pulping of corn stalks. The corn stalks come from unprotected corn plantations and were gathered from the Iasi region, Romania with the permission of the farmers, following the national rules for agricultural waste collection. In a typical pulping experiment, about 400 [g] oven dried stalks were used. The material was pulped with 48 [g] NaOH and 3600 [cm^3] distilled water (corresponding to

12% NaOH alkali charge and a solid to liquid ratio of 1:9). Following reactor closing, heating was started to reach a temperature of 120 [°C] (25 [min]) which was maintained for 40 [min] After pulping time was completed, a sample of the liquid phase was withdrawn from the pulping reactor, cooled to room temperature and filtered to remove any remaining solids. The resulted liquor had a characteristic darkish brown color, a relatively high alkalinity (pH =11) a conductivity of 24.5 [mS/cm] and organic load (COD = 40 [g O_2/L]). The solid content of the black liquor was further determined according to the TAPPI test method (TAPPI T650, 1989). Organic to inorganic ratio was determined taking into account the ash content values (TAPPI 625 cm – 85).

Common commercial TiO_2 powder (M-1319) supplied at FCC purity grade by Mayam *(http://www.mayam.eu)* was used as such during this study. The powder was characterized by SEM and EDX analysis and, in a previous study, was successfully applied for photochemical degradation of methylene blue (Atomi et al. 2018).

The experiments were performed using irregular shape particles of active carbon supplied by Buzău Romcarbon Company (Romania), active carbon that was characterized in the study of (Secula et al. 2011) : specific microporous volume 0.48 [cm^3/g], total microporous volume 0.66 [cm^3/g], mean pore size 1.62 [nm], BET surface 1403 [m^2/g], external surface 38 [m^2/g] and total surface 631 [m^2/g]. Prior to the experimental study, the particles were classified by sieving, the average diameter ranging among 2.5 and 3.15 [mm].

2.2 Equipment

The UV light source was a Biocomp UV-lamp with wavelength of 253.7± 0.8 [nm]. An analog UV light sensor GUVA S12SD was used to measure the intensity of incident UV radiation. The UV-vis spectra and the absorbance values were recorded using a JASCO V-550 UV-Vis spectrophotometer. The chemical oxygen demand (COD), [mg O_2/L] was measured using a standard Hach-Lange kit LCK 114. A BHG Hermle Z 229 Centrifuge: 220 V, 50 Hz, 1.1 A, 240 W, maximum number of revolutions 15000 rpm was also used.

2.3 Experimental design

In order to determine the optimal parameters for BL decolorization three representative independent variables were considered for each method, as depicted in Table 1. These parameters and their limits were selected based the data provided by literature (Peralta-Zamora et al. 1998). Following the design of experiments approach (DOE) proposed by Box and Hunter (Box and Hunter 1957) a minimum number of experiments were statistically programmed as presented in Table 2, where η_{ACD} (%) represents the decolorization efficiency for the active carbon decolorization and η_{PCD} (%) for the TiO2 promoted photochemical decolorization. In table 2 both the coded and the decoded variables were presented, the

notations being the same as one used in Table 1. The bold columns from Table 2 indicate the experimental results obtained with the identified values by the DOE approach.

Table 1

Designated variables and their variation range for the chosen decolorization methods

Active carbon decolorization (ACD)					
Independent variables	**Measure units**	**Notation**	**Range**		**Symbol**
			from	**to**	
Active carbon concentration	[g/L]	$[AC]_{x1}$	5	50	[AC]
Dilution	ratio	$[Ct]_{x2}$	1:100	1:200	[Dil]
Contact time	[min]	$[Dil]_{x3}$	10	30	[Ct]
TiO_2 promoted photochemical decolorization (PCD)					
Independent variables	**Measure units**	**Notation**	**Range**		**Symbol**
			from	**to**	
TiO_2 concentration	[g/L]	$[TiO_2]_{x1}$	1	2	$[TiO_2]$
UV path length	[cm]	$[lt]_{x2}$	5	25	[hUV]
Irradiation time	[min]	$[hUV]_{x3}$	15	60	[lt]

Table 2

Experiment planning and results

No.	Coded variable			Decoded ACD			Decoded PCD			η_{ACD} (%)	η_{PCD} (%)
	x_1	x_2	x_3	$[AC]_{x1}$	$[Ct]_{x2}$	$[Dil]_{x3}$	$[TiO_2]_{x1}$	$[It]_{x2}$	$[hUV]_{x3}$		
1	1	1	1	50	30	200	2	60	25	**83.08**	**19.83**
2	−1	1	1	5	30	200	1	60	25	**57.40**	**20.62**
3	1	−1	1	50	10	200	2	15	25	**69.74**	**16.88**
4	−1	−1	1	5	10	200	1	15	25	**33.54**	**18.41**
5	1	1	−1	50	30	100	2	60	5	**81.22**	**33.90**
6	−1	1	−1	5	30	100	1	60	5	**52.27**	**36.63**
7	1	−1	−1	50	10	100	2	15	5	**60.68**	**18.50**
8	−1	−1	−1	5	10	100	1	15	5	**21.48**	**20.45**
9	α	0	0	54.8	20	150	2.11	37.5	15	**80.53**	**19.39**
10	−α	0	0	0.176	20	150	0.89	37.5	15	**13.99**	**24.90**
11	0	α	0	27.5	32.15	150	1.5	64.8	15	**78.58**	**19.52**
12	0	−α	0	27.5	7.85	150	1.5	10.15	15	**65.70**	**17.23**
13	0	0	α	27.5	20	210.75	1.5	37.5	27.15	**72.65**	**18.61**
14	0	0	−α	27.5	20	89.25	1.5	37.5	2.85	**74.24**	**35.01**
15	0	0	0	27.5	20	150	1.5	37.5	15	**68.88**	**18.74**
16	0	0	0	27.5	20	150	1.5	37.5	15	**69.28**	**19.52**

2.4 Experimental procedure

The BL was used as such, underprivileged of any pH chemical regulations, at room temperature. Bi-distilled water was used to reach the required dilution ratio for each experiment. In order to avoid settling (and to ensure a constant exposure of the mixture) the slurry was stirred constantly during all the experiments involving the presence of TiO_2 powder or active carbon particles.

In the case of active carbon decolorization, for a well-defined period of time, 100 [mL] samples of specifically diluted BL solutions were mixed with the adequate amount of active carbon, according to the data presented in Table 2. Disposable disc filters 0.45 [μm] were used for particles separation.

In the case of TiO_2 promoted photochemical decolorization, 50 [mL] samples of BL solutions (with 1:100 dilution ratio) were mixed with the adequate amount of TiO_2 and placed below the UV source for the corresponding period of time. After irradiation, the TiO_2 powder was separated from the solutions using a centrifugal separator. The required UV path length that gives the intensity of the incident UV radiation was attained by changing the distance between the UV source and the sample under study.

2.5 Chemical assays

The BL decolorization was checked by measuring the absorbance of the solution given by the lignin content at 280 [nm] (UV_{280}) as presented in Fig. 1. The correlation between the chemical oxygen demand (COD) and the absorbance was determined at different dilution ratio in order to establish a calibration curve that validates the accuracy of decolorization efficiency calculations. The coefficient of determination (R^2) was 0.97, in accordance with the literature reported values (Torrades et al. 2011). The efficacy of BL decolorization was calculated using the following equation:

$$\eta\,(\%) = \frac{[UV_{280}]_0 - [UV_{280}]}{[UV_{280}]_0} \cdot 100 \qquad (1)$$

where and are the absorbance's recorded before and after each experiment.

2.6 Software and algorithm

The MINITAB package (Minitab Institute, USA) was chosen to implement the response surface method algorithm. In addition, the process was optimized with a second method represented by DE, an efficient metaheuristic approach, that was successfully used (simple or in combination with other approaches) for optimization and modelling of a wide range of systems, from robot control (Neri and Mininno 2010), water quality monitoring (Yazdi 2018), adsorption processes (Bleotu et al. 2018). Examples of DE application in chemical engineering can be found in (Dragoi and Curteanu 2016). The DE based software used was developed in (Drăgoi et al. 2012) in combination with artificial neural networks (ANNs) and applied for predicting the liquid crystalline property of some organic compounds. Distinctively, in this work, the ANN is replaced by the model determined with MINITAB package, the DE variant (SADE) performing only the process optimization part.

DE is inspired from the Darwinian principle of evolution (Storn and Price 1995) and it works with a population of potential solutions that it is evolved (through a series of steps that include mutation, crossover and selection) until a stop criterion is reached. After the potential solutions (which will be further referred as individuals) are initialized (using a random based procedure), the individuals undergo a mutation procedure. DE has many mutation variants and, in this work, two differential terms combined

with a randomly selected based vector was used (this is also known as the rand/2 version). Eq. 2 describes the mutation equation used.

$$\omega_i = \alpha + F \cdot (\beta + \gamma) \quad (2)$$

where *a* is the base vector, *F* is the scaling factor (one of the control parameters of DE), and *b, γ* are the differential terms. The differential term is created by subtracting a randomly selected vector with another one.

After that, the features of the mutated and current individuals are combined to create a new population called trial. This is the crossover step and the variant used in this work is the binomial crossover.

In the next step, the trial and the current population undergo a one-to-one comparison, the best individuals being selected to form the next generation. The measure used to determine the best individuals is represented by the fitness function and for the current work, the fitness function represents the regression model of the process generated by the Minitab software.

One of the main characteristics of the SADE version is represented by the use of self-adaptability to determine the values of the control parameters. In this manner, the difficult task of manually setting the optimal values for the control parameters is automatized by including them into the algorithm itself. A simplified schema of approach used in this work is presented in Fig. 2.

3. Results And Discussion

3.1. ACD vs PCD

Evidently, the basic principles of the BL decolorization methods selected for this study makes a comparison attempt to be rather impractical. Furthermore, the chosen parameters and their range of variation make the straightforward comparison between ACD and PCD quite difficult.

However, from the experimental data obtained on the samples with the dilution ratio (1:100) used for both methods (the experiments from 5 to 8 in Table 2) the superiority of ACD is clearly established. The results are comparable in one case only, for the experimental data set no. 8, when the values for the ACD and PCD parameters were set for minimum values. Evidently, in terms of decolorization efficiency, the ACD method exhibits better performances (83.08% vs. 36.63%).

When it comes to PCD, it should be mentioned that, commonly, the method involves the use of additional chemical oxidants: Fenton's reagent, hydrogen peroxide and other combinations that favours the formation of OH radicals and other short-lived radical species, which highly elevates the methods efficacy. However, no additional chemicals (reagents, pH regulators) were used during this study, since our goal was not necessary to compare two well-known methods but to use and apply classic and

modern optimization techniques in order to find their optimal parameters. Therefore, no claim that one method is better than the other will conclude our work.

3.2. Response Surface Method

A full second-order polynomial model was obtained by multiple regression technique for three parameters using the MINITAB package. The regression equations in terms of actual factors (uncoded units) for the ACD method is presented below:

$$\eta_{ACD}\ (\%) = 0.2 + 2.833\cdot[AC] + 1.59\cdot[Ct] - 0.124\cdot[Dil] - 0.03073\cdot[AC]^2 + 0.0130\cdot[Ct]^2 +$$

$$+ 0.00087\cdot[Dil]^2 - 0.0143\cdot[AC]\cdot[Ct] - 0.00014\cdot[AC]\cdot[Dil] - 0.00478\cdot[Ct]\cdot[Dil] \qquad (3)$$

By setting one parameter at a constant value, the median value of the interval of variation, three dimensional plots (surface plots) were drawn as presented in Figs. 3A, 3B and 3C. Displaying the parameter variation in such manner allows the visualization of maximum and/or minimum points that leads to accurate identification of the optimal values and shows the influence of the selected parameters over the BL decolorization efficiency.

The response surface plots showing the evolution of the decolorization efficiency as a function of contact time and active carbon concentration at constant dilution ration 1:150 is displayed in Fig. 3A. As expected, the increasing of both [Ct] and [AC] have a substantial influence on the efficiency, its maximum value (over 75%) being reached after 30 [min] at 40 [g/L] adsorbent concentration. Fig. 3B shows the influence of dilution ratio and active carbon concentration towards decolorization efficiency after 20 [min] of contact time. The maximum value of decolorization efficiency was reached at the highest [Dil] value 1:200 in presence of 40 [g/L] active carbon. When [AC] was held constant at 27.5 [g/L] the efficiency reached nearly 95% after 30 [min] for [Dil] of 1:200 as presented in Fig. 3C.

The RSM predicted values equivalent with the solution sets of the regression equation stretch the optimal values for the ACD variable parameters. The best five sets of Minitab optimization results based on the regression equation are presented in Table 3. For all the optimization data provided in each case, two solutions were experimentally validated in order to confirm the results.

Table 3

The RSM optimization for active carbon decolorization of BL

Solution no.	[AC], [g/L]	[Ct], [min]	[Dil], ratio	$\eta_{ACD,}$ (%)-predicted	η_{ACD}, (%)-experimental
1	38.43	32.15	89.25	92.24	92.3
2	38.12	32.15	210.75	89.70	91.1
3	47.53	32.15	89.25	89.68	-
4	37.32	32.15	210.75	89.68	-
5	29.77	31.95	89.65	89.59	-

The regression equations in terms of actual factors (uncoded units) for the PCD method is presented in Eq 4. In Figs. 4A, 4B and 4C the variation of BL decolorization efficiency for PCD as a function of two variables is displayed.

$$\eta_{PCD}\,(\%) = 33.0 - 16.3\cdot[TiO_2] + 0.600\cdot[It] - 1.299\cdot[hUV] + 4.30\cdot[TiO_2]^2 - 0.00292\cdot[It]^2 + 0.0424\cdot[hUV]^2 - 0.000\cdot[TiO_2]\cdot[It] + 0.059\cdot[TiO_2]\cdot[hUV] - 0.01468\cdot[It]\cdot[hUV] \quad (4)$$

The response surface plots showing the evolution of the decolorization efficiency as a function of irradiation time and TiO_2 concentration at constant UV path length of 15 [cm] is displayed in Fig. 4A. It can be noticed that the efficiency rises with the increase of [It] and it is higher at lower values of [TiO_2]. The surface plot in Fig. 4B shows the influence of TiO_2 concentration and UV path length after 37.5 [min] of irradiation. Once more, the efficiency is higher at lower values of [TiO_2] and tends to increase with the decrease of [hUV]. When the [TiO_2] were held constant at 1.5 [g/L] as presented in Fig. 4C, the efficiency growths with the increase of irradiation time and with the decrease of the UV path length.

The best five sets of results for the Minitab optimization based on the regression equation are presented in Table 4.

Table 4

The RSM optimization results for PCD of BL

Solution no.	[TiO_2], [g/L]	[It], [min]	[hUV], [cm]	$\eta_{PCD,}$ (%)-predicted	η_{PCD}, (%)-experimental
1	0.89	64.84	2.85	42.57	43.2
2	2.10	64.84	2.85	38.64	38.8
3	0.89	45.46	2.85	37.99	-
4	0.89	36.39	27.15	22.71	-
5	0.89	27.59	27.15	22.59	-

3.3. Differential evolution

In order to determine the optimal configuration of parameters leading to the maximization η_{PCD}, (%) for both PCD and ACD approaches, DE in combination with the regression equations generated by Minitab (Eqs. 3-4) was applied. The settings used for DE optimization were: number of individuals in the population=30, number of iterations=50. The control parameters values were automatically adjusted by the software using a self-adaptive procedure (Drăgoi et al. 2012). These values were selected based on the author's expertise and practical aspects, as the number of parameters included into the optimization process is the same as the number of process parameters considered in the modelling phase: [AC], [Ct], [Dil] (for ACD) and [TiO_2], [It], [hUV] (for PCD).

The DE based optimization procedure, for both PCD and ACD was applied in three cases: i) the limits of the operating conditions were the same as in the experimental data (Case 1); ii) the limits were extended to ±20% (extrapolation) (Case 2); and iii) the amount of active reagents added was limited (1-20 [g/L] activated carbon for ACD and 0.4-1 [g/L] TiO_2 for PCD) (Case 3). Five solutions obtained for these three cases are listed in Tables 5 and 6. It is worth mentioning that, due to the random nature of the DE base algorithm, at each run, different solutions can be obtained. Therefore, DE is not limited by a pre-specified number of solutions and can provide various configurations that lead to very similar results.

Table 5

DE optimization results for ACD of BL

Case	Solution no.	[AC], [g/L]	[Ct], [min]	[Dil], ratio	$\eta_{ACD,}$ (%)-predicted	η_{ACD}, (%)-experimental
Case 1	1	19.07	47.51	169.59	100	99.03
	2	36.3	41	138.16	100	-
	3	25.87	42.6	131.24	100	-
	4	31.27	39.15	104.08	99.98	-
	5	7.29	52.42	121.7	99.97	98.87
Case 2	1	56.76	50.48	134.08	100	97.42
	2	32.21	42.92	191.68	100	-
	3	25.94	43.69	152.67	100	-
	4	19.46	46.83	157.38	99.97	-
	5	55.7	48.1	120.17	99.95	98.24
Case 3	1	4.84	55.18	135.77	100	98.76
	2	8.98	54.14	172.91	100	-
	3	12.34	50.02	137.35	100	-
	4	17.99	46.49	135.48	100	-
	5	19.99	47.38	183.31	99.98	98.69

Table 6

DE optimization results for PCD of BL

Case	Solution no.	[TiO_2], [g/L]	[It], [min]	[hUV], [cm]	$\eta_{PCD,}$ (%)-predicted	η_{PCD}, (%)-experimental
Case 1	1	0.89	59.99	2.85	41.64	40.84
	2	0.90	58.83	3.03	40.98	-
	3	0.90	57.74	2.96	40.88	-
	4	0.99	59.82	3.04	40.45	-
	5	1.10	57.74	3.33	38.70	36.42
Case 2	1	0.71	71.98	2.28	46.58	45.98
	2	0.72	68.42	2.30	45.88	-
	3	0.75	70.08	2.34	45.77	-
	4	0.78	69.11	2.46	45.08	-
	5	0.87	69.03	3.41	42.34	42.4
Case 3	1	0.40	59.99	2.85	46.83	46.22
	2	0.49	57.28	2.88	45.09	-
	3	0.48	55.41	3.57	43.53	-
	4	0.43	48.59	3.11	43.26	-
	5	0.56	54.91	3.65	42.35	41.75

As it can be observed from the experimental validation, there is an acceptable error between the predictions and the actual values. In addition, compared with the solutions provided by the RSM approach, DE is able to find optimal values in a wide range of combinations. For example, for the CD process, in case 1, the process efficiency varies between 99.97 and 100%, while the values for the identified parameters varies between [7.29, 31.27] for [AC], [41, 52.42] for [Ct] and [104.08, 169.59] for [Dil]. This implies that the efficiency function is multimodal and that that there are multiple combinations for the parameters values that lead to the same result. Taking into consideration the economic aspect, the process optimization is transformed from a uni-objective (maximum efficiency) to a multi-objective problem (highest efficiency with the minimum of resources consumed).

4. Conclusions

Active carbon decolorization and TiO_2 promoted photochemical decolorization of black liquor obtained from laboratory pulping of corn stalks was experimentally studied. Three variable parameters were considered for each method: dilution ratio, active carbon concentration and contact time for ACD, respectively TiO_2 concentration, UV path length (irradiation intensity) and irradiation time for PCD. The

number of the experiments performed in order to establish the optimal working parameters for each decolorization technique were statistically programmed following the design of experiments approach. In addition, the two processes were modelled and optimized using RSM and DE. In both cases, the optimization results were experimentally validated. Compared with RSM, the DE based approach is more flexible (allows a wide variety of limits and or/extrapolations set to the parameters) and it is better at exploring the search space, being able to determine multiple combinations of solutions leading to similar outputs. Moreover, for active carbon, an improvement from 81.27% to 100% and for TiO2-based degradation from 36.63% to 46.83% was obtained, proving that the application of state-of-the-art computational approaches can lead to significant improvements and that they can be efficiently used raise performance of various decolorization processes.

Declarations

Funding:

This work was supported by project PN-III-P4-ID-PCE no 58/2021 financed by UEFISCDI, Romania

Conflict of interests:

On behalf of all authors, the corresponding author states that there is no conflict of interest.

Availability of data and material:

All the data this manuscript is based on is presented in the text, tables and figures.

Code availability:

https://elenadragoi.ro/CV/Documents/AITB-%20ANN_DE.7z

Acknowledgements

This work was supported by project PN-III-P4-ID-PCE no 58/2021 financed by UEFISCDI, Romania

References

1. Atomi, A. I., Suditu, G. D., Puiţel, A. C. & Nechita, M. T. Experimental study on tio2 promoted photo-degradation of methylene blue. *Bulletin of Romanian Chemical Engineering Society*, **5**, 68–74 (2018).

2. Azadi Aghdam, M., Kariminia, H-R. & Safari, S. Removal of lignin, cod, and color from pulp and paper wastewater using electrocoagulation. *Desalination and Water Treatment*, **57**, 9698–9704 https://doi.org/10.1080/19443994.2015.1040461 (2016).
3. Baycan Parilti, N. & Akten, D. Optimization of tio2/fe(iii)/solar uv conditions for the removal of organic contaminants in pulp mill effluents., **265**, 37–42 https://doi.org/10.1016/j.desal.2010.07.027 (2011).
4. Bleotu, I., Dragoi, E. N., Mureşeanu, M. & Dorneanu, S-A. Removal of cu(ii) ions from aqueous solutions by an ion-exchange process: Modeling and optimization. *Environ. Prog. Sustain. Energy*, **37**, 605–612 https://doi.org/10.1002/ep.12793 (2018).
5. Box, G. E. P. & Hunter, J. S. Multi-factor experimental designs for exploring response surfaces. *The Annals of Mathematical Statistics*, **28**, 195–241 (1957).
6. Chang, C-N. *et al.* Decolorizing of lignin wastewater using the photochemical uv/tio2 process., **56**, 1011–1017 https://doi.org/10.1016/j.chemosphere.2004.04.021 (2004).
7. Darvishmotevalli, M., Zarei, A., Moradnia, M., Noorisepehr, M. & Mohammadi, H. Optimization of saline wastewater treatment using electrochemical oxidation process: Prediction by rsm method. *MethodsX*, **6**, 1101–1113 https://doi.org/10.1016/j.mex.2019.03.015 (2019).
8. De los Santos Ramos, W., Poznyak, T., Chairez, I. & Córdova, R. I. Remediation of lignin and its derivatives from pulp and paper industry wastewater by the combination of chemical precipitation and ozonation. *Journal of Hazardous Materials*, **169**, 428–434 https://doi.org/10.1016/j.jhazmat.2009.03.152 (2009).
9. Drăgoi, E-N., Curteanu, S. & Lisa, C. A neuro-evolutive technique applied for predicting the liquid crystalline property of some organic compounds. *Eng. Optim*, **44**, 1261–1277 https://doi.org/10.1080/0305215x.2011.644546 (2012).
10. Dragoi, E. N. & Curteanu, S. The use of differential evolution algorithm for solving chemical engineering problems. *Reviews in Chemical Engineering*, **32**, 149–180 https://doi.org/10.1515/revce-2015-0042 (2016).
11. Ganjidoust, H., Tatsumi, K., Yamagishi, T. & Gholian, R. N. Effect of synthetic and natural coagulant on lignin removal from pulp and paper wastewater. *Water Science and Technology*, **35**, 291–296 https://doi.org/10.1016/S0273-1223(96)00943-2 (1997).
12. Garg, A., Mishra, I. M. & Chand, S. Catalytic wet oxidation of the pretreated synthetic pulp and paper mill effluent under moderate conditions., **66**, 1799–1805 https://doi.org/10.1016/j.chemosphere.2006.07.038 (2007).
13. Garg, A., Mishra, I. M. & Chand, S. Effectiveness of coagulation and acid precipitation processes for the pre-treatment of diluted black liquor. *Journal of Hazardous Materials*, **180**, 158–164 https://doi.org/10.1016/j.jhazmat.2010.04.008 (2010).
14. Ghasemi, S. *et al.* Design, operation, performance evaluation and mathematical optimization of a vermifiltration pilot plan for domestic wastewater treatment. *Journal of Environmental Chemical Engineering*, **8**, 103587 https://doi.org/10.1016/j.jece.2019.103587 (2020).

15. Kansal, S. K., Singh, M. & Sud, D. Studies on tio2/zno photocatalysed degradation of lignin. *Journal of Hazardous Materials*, **153**, 412–417 https://doi.org/10.1016/j.jhazmat.2007.08.091 (2008).
16. Kim, S-C. Application of response surface method as an experimental design to optimize coagulation–flocculation process for pre-treating paper wastewater. *Journal of Industrial and Engineering Chemistry*, **38**, 93–102 https://doi.org/10.1016/j.jiec.2016.04.010 (2016).
17. Kloch, M. & Toczyłowska-Mamińska, R. Toward optimization of wood industry wastewater treatment in microbial fuel cells—mixed wastewaters approach. *Energies*, **13**, 263 (2020).
18. Kreetachat, T. *et al.* Effects of ozonation process on lignin-derived compounds in pulp and paper mill effluents. *Journal of Hazardous Materials*, **142**, 250–257 https://doi.org/10.1016/j.jhazmat.2006.08.011 (2007).
19. Ksibi, M. *et al.* Photodegradation of lignin from black liquor using a uv/tio2 system. *Journal of Photochemistry and Photobiology A: Chemistry*, **154**, 211–218 https://doi.org/10.1016/S1010-6030(02)00316-7 (2003).
20. Merayo, N., Hermosilla, D., Blanco, L., Cortijo, L. & Blanco, Ã. Assessing the application of advanced oxidation processes, and their combination with biological treatment, to effluents from pulp and paper industry. *Journal of Hazardous Materials*, **262**, 420–427 https://doi.org/10.1016/j.jhazmat.2013.09.005 (2013).
21. Mirjalili, S. *et al.* Salp swarm algorithm: A bio-inspired optimizer for engineering design problems. *Adv Eng Soft*, **114**, 163–191 https://doi.org/10.1016/j.advengsoft.2017.07.002 (2017).
22. Mohan, S. V. & Karthikeyan, J. Removal of lignin and tannin colour from aqueous solution by adsorption onto activated charcoal. *Environ. Pollut*, **97**, 183–187 https://doi.org/10.1016/S0269-7491(97)00025-0 (1997).
23. Neri, F. & Mininno, E. Memetic compact differential evolution for cartesian robot control. *IEEE Computational Intelligence Magazine*, **5**, 54–65 https://doi.org/10.1109/Mci.2010.936305 (2010).
24. Panepinto, D. *et al.* (2020) Optimization of the wastewater treatment plant: From energy saving to environmental impact mitigation. Frontiers in water-energy-nexus—nature-based solutions, advanced technologies and best practices for environmental sustainability.Springer.
25. Peralta-Zamora, P. *et al.* Evaluation of zno, tio2 and supported zno on the photoassisted remediation of black liquor, cellulose and textile mill effluents., **36**, 2119–2133 https://doi.org/10.1016/S0045-6535(97)10074-1 (1998).
26. Secula, M. S., Cagnon, B., Cretescu, I., Diaconu, M. & Petrescu, S. Removal of an acid dye from aqueous solutions by adsorption on a commercial granular activated carbon: Equilibrium, kinetic and thermodynamic study. *Scientific Study & Research. Chemistry & Chemical Engineering, Biotechnology, Food Industry*, **12**, 307 (2011).
27. Shankar, R., Singh, L., Mondal, P. & Chand, S. Removal of cod, toc, and color from pulp and paper industry wastewater through electrocoagulation. *Desalination and Water Treatment*, **52**, 7711–7722 https://doi.org/10.1080/19443994.2013.831782 (2014).

28. Shomar, B., Al-Darwish, K. & Vincent, A. Optimization of wastewater treatment processes using molecular bacteriology. *Journal of Water Process Engineering*, **33**, 101030 https://doi.org/10.1016/j.jwpe.2019.101030 (2020).
29. Storn, R. P. K. *Differential evolution - a simple and efficient adaptive scheme for global optimization over continuous spaces* (Berkley, 1995).
30. Subramonian, W., Wu, T. Y. & Chai, S-P. Photocatalytic degradation of industrial pulp and paper mill effluent using synthesized magnetic fe2o3-tio2: Treatment efficiency and characterizations of reused photocatalyst. *Journal of Environmental Management*, **187**, 298–310 https://doi.org/10.1016/j.jenvman.2016.10.024 (2017).
31. Torrades, F., Saiz, S. & García-Hortal, J. A. Using central composite experimental design to optimize the degradation of black liquor by fenton reagent., **268**, 97–102 https://doi.org/10.1016/j.desal.2010.10.003 (2011).
32. Ugurlu, M., Gurses, A., Yalcin, M. & Dogar, C. Removal of phenolic and lignin compounds from bleached kraft mill effluent by fly ash and sepiolite. *Adsorption*, **11**, 87–97 https://doi.org/10.1007/s10450-005-1096-6 (2005).
33. Wang, J. *et al.* Multivariate optimization of the pulse electrochemical oxidation for treating recalcitrant dye wastewater. *Separation and Purification Technology*, **230**, 115851 https://doi.org/10.1016/j.seppur.2019.115851 (2020).
34. Yazdi, J. Water quality monitoring network design for urban drainage systems, an entropy method. *Urban Water Journal*, **15**, 227–233 https://doi.org/10.1080/1573062X.2018.1424215 (2018).
35. Zaied, M. & Bellakhal, N. Electrocoagulation treatment of black liquor from paper industry. *Journal of Hazardous Materials*, **163**, 995–1000 https://doi.org/10.1016/j.jhazmat.2008.07.115 (2009).
36. Zhang, M., Dong, H., Zhao, L. & Wang, D. A review on fenton process for organic wastewater treatment based on optimization perspective. *Science of The Total Environment*, **670**, 110–121 https://doi.org/10.1016/j.scitotenv.2019.03.180 (2019).
37. Zhang, Q. & Chuang, K. T. Adsorption of organic pollutants from effluents of a kraft pulp mill on activated carbon and polymer resin. *Advances in Environmental Research*, **5**, 251–258 https://doi.org/10.1016/S1093-0191(00)00059-9 (2001).
38. Zhou, X., Hou, Z., Lv, L., Song, J. & Yin, Z. Electro-fenton with peroxi-coagulation as a feasible pre-treatment for high-strength refractory coke plant wastewater: Parameters optimization, removal behavior and kinetics analysis., **238**, 124649 https://doi.org/10.1016/j.chemosphere.2019.124649 (2020).

Figures

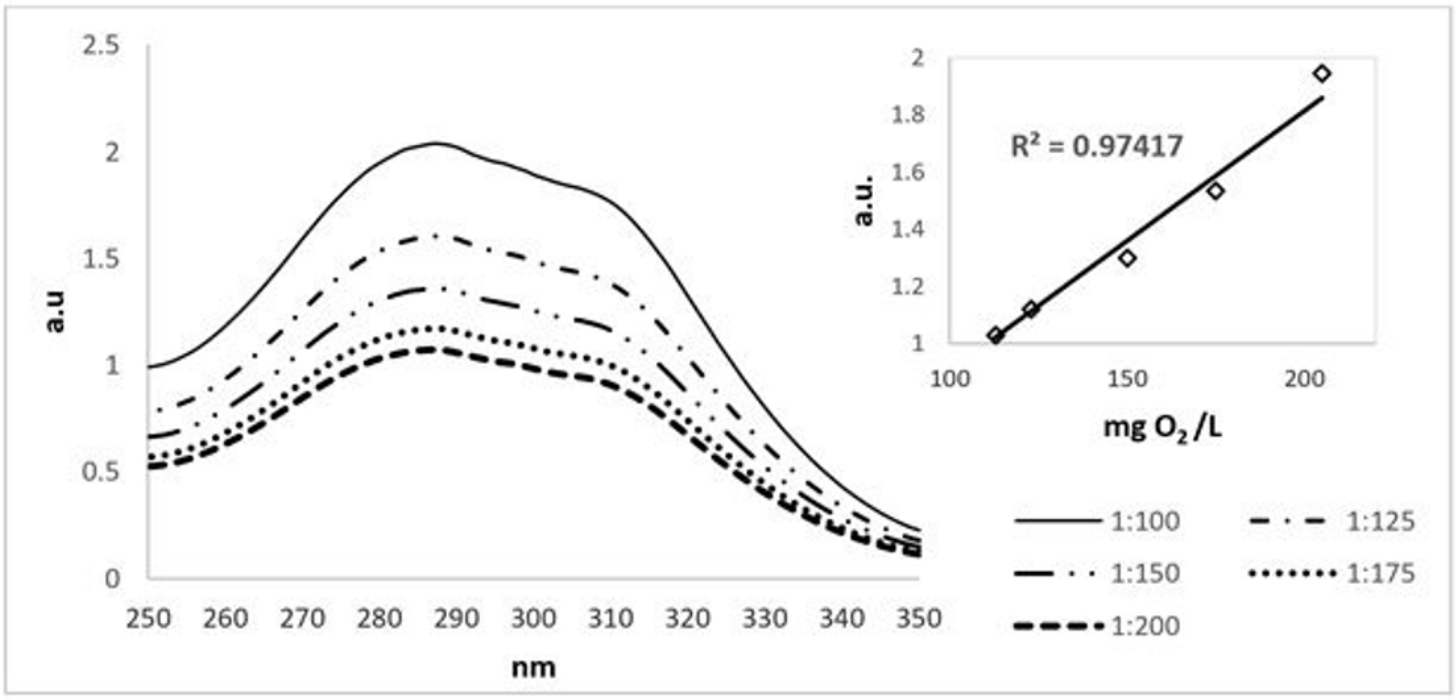

Figure 1

UV-VIS spectra of BL at different dilution ratio. The inset displays the correlation between the chemical oxygen demand (COD) and the absorbance at the corresponding dilution.

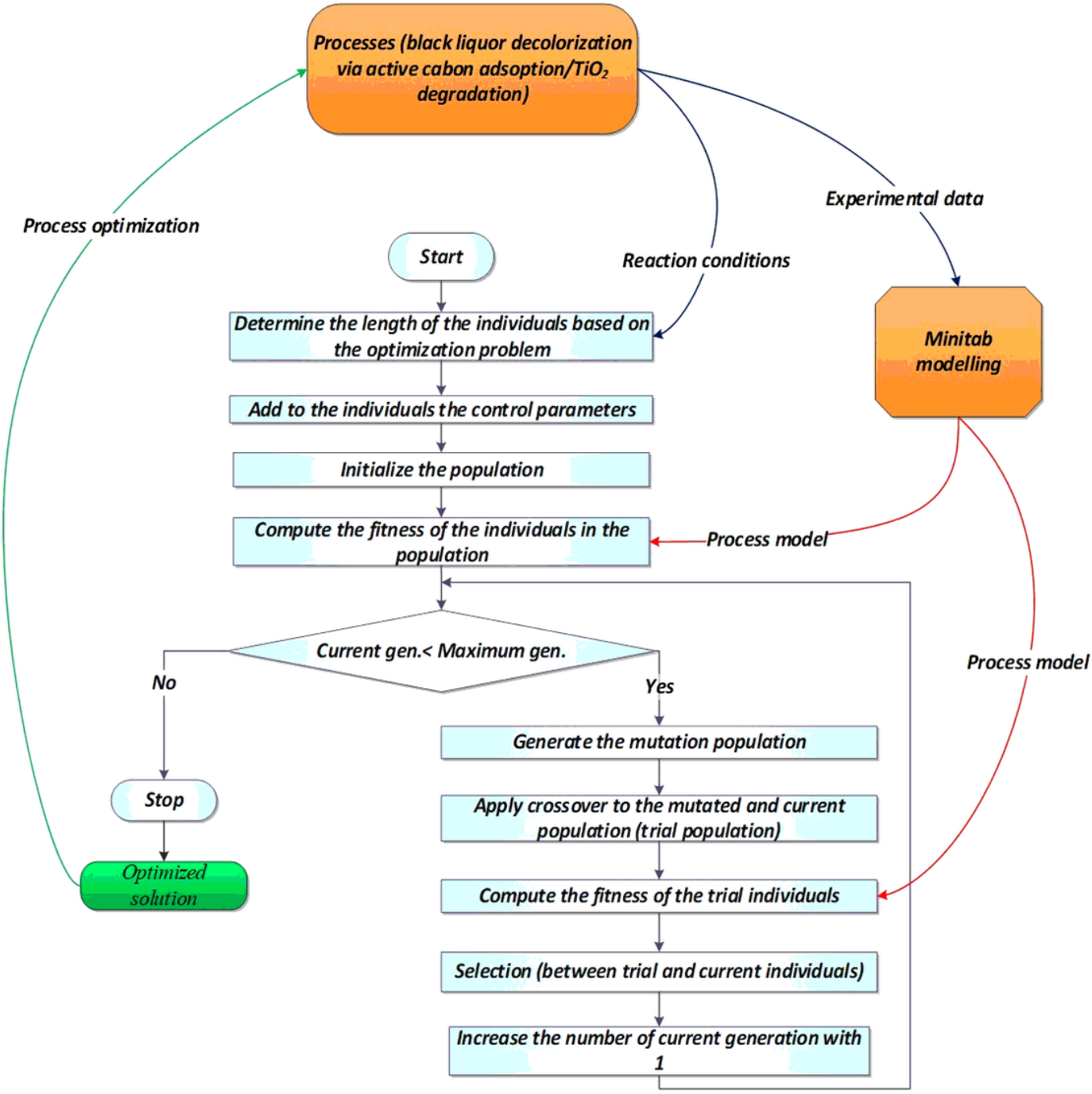

Figure 2

Scheme of the overall optimization procedure.

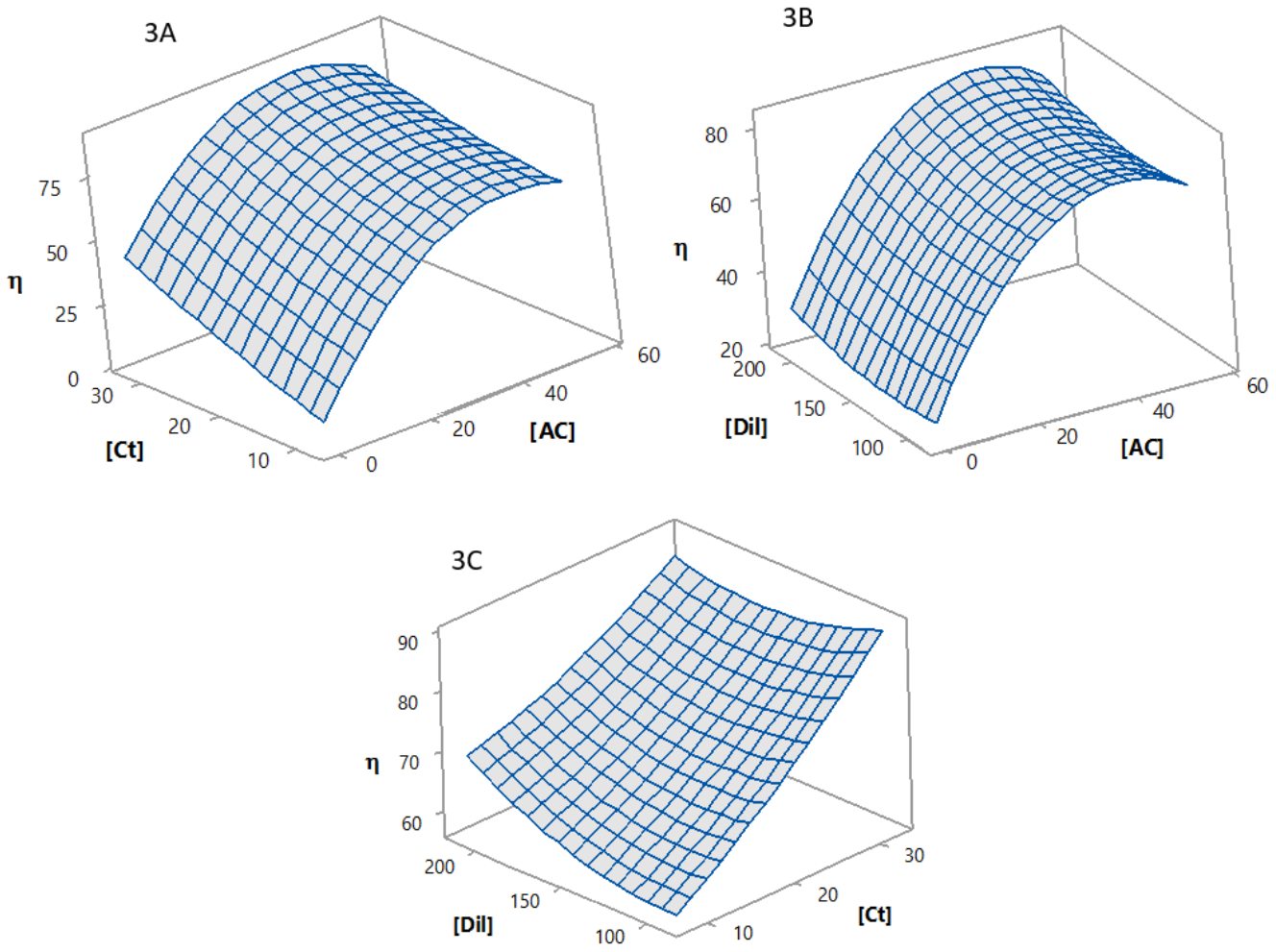

Figure 3

3A. Surface plot efficiency vs [Ct] and [AC], at [Dil] = 1:150; 3B. Surface plot efficiency vs [Dil] and [AC],at [Ct] = 20 [min]; 3C. Surface plot efficiency vs [Dil] and [Ct], at [AC] = 27.5 [g/L]

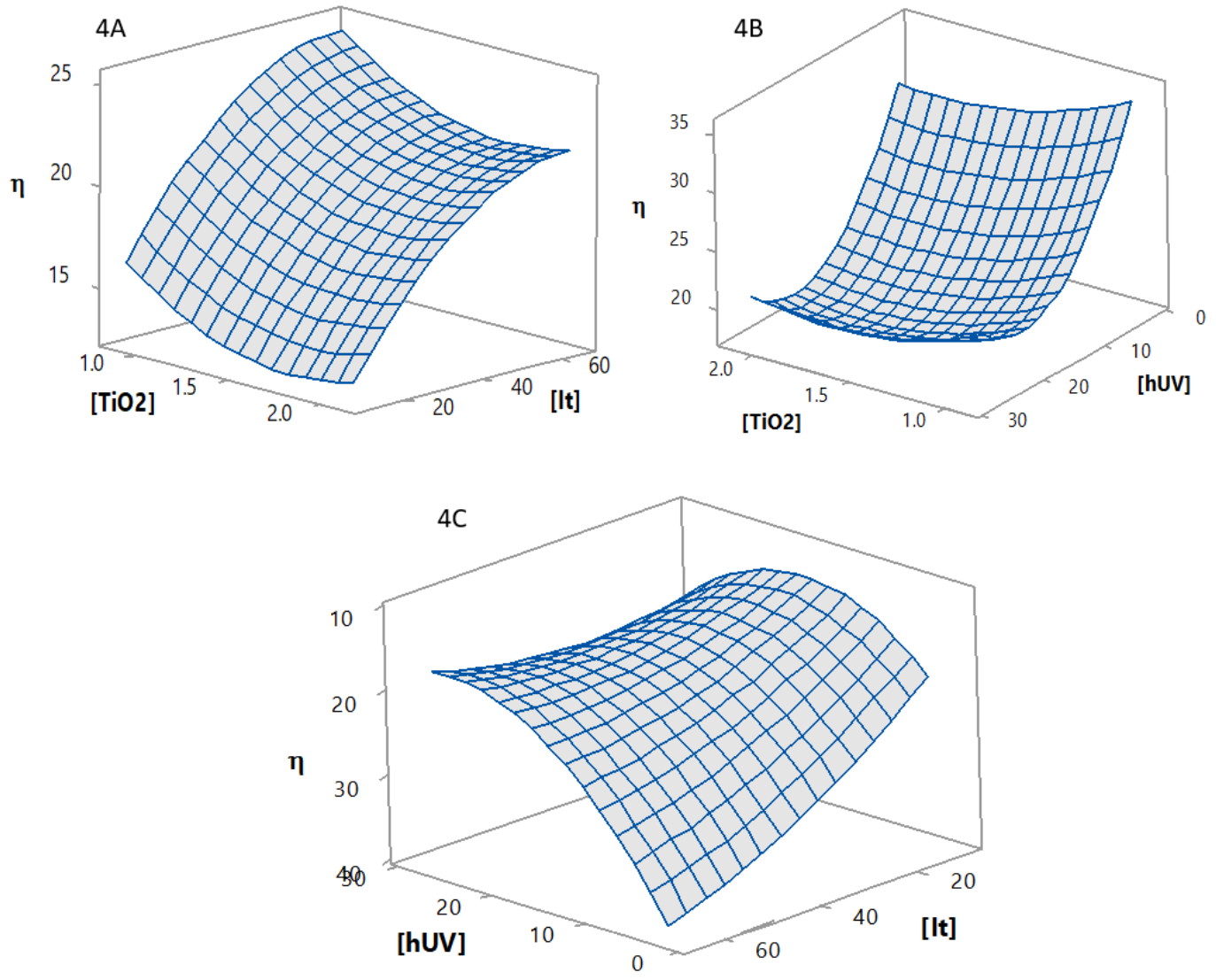

Figure 4

4A. Surface plot efficiency vs [It] and [TiO2], at [hUV] = 15 [cm]; 4B. Surface plot efficiency vs [hUV] and [TiO2],at [It] = 37.5 [min]; 4C. Surface plot efficiency vs [It] and [hUV], at [TiO2] = 1.5 [g/L]